This is an *Accepted Manuscript*, which has been through the Royal Society of Chemistry peer review process and has been accepted for publication.

Accepted Manuscripts are published online shortly after acceptance, before technical editing, formatting and proof reading. Using this free service, authors can make their results available to the community, in citable form, before we publish the edited article. We will replace this *Accepted Manuscript* with the edited and formatted *Advance Article* as soon as it is available.

You can find more information about *Accepted Manuscripts* in the **Information for Authors**.

Dalton Transactions

ARTICLE

Ab initio Structure Determination of Interlayer Expanded Zeolites by Single Crystal Rotation Electron Diffraction

Peng Guo,[a] Leifeng Liu,[a] Yifeng Yun,[a] Jie Su,[a] Wei Wan,[a] Hermann Gies,[b] Haiyan Zhang,[c] Feng-Shou Xiao,[c] Xiaodong Zou*[a]

Layered solids often form thin plate-like crystals that are too small to be studied by single-crystal X-ray diffraction. Although powder X-ray diffraction (PXRD) is the conventional method to study such solids, it has limitations because of peak broadening and peak overlapping. We have recently developed software-based rotation electron diffraction (RED) method for automated collection and processing of 3D electron diffraction data. Here we demonstrate the *ab initio* structure determination of two interlayer expanded zeolites, the microporous silicates COE-3 and COE-4 (COE-n stands for International Network of Centers of Excellence-n), from submicron-sized crystals by the RED method. COE-3 and COE-4 are built of ferrierite-type layers pillared by (-O-Si(CH$_3$)$_2$-O-) and (-O-Si(OH)$_2$-O-) linker groups, respectively. The structures contain 2D intersecting 10-ring channels running in parallel to the ferrierite layers. Because both COE-3 and COE-4 are electron-beam sensitive, a combination of RED datasets from 2-3 different crystals was needed for the structure solution and subsequent structure refinement. The structures were further refined by Rietveld refinement against the PXRD data. The structure models obtained from RED and PXRD were compared.

Introduction

Zeolites are interesting due to their wide applications in catalysis, adsorption and ion exchange.[1] However, the applications are limited by the pore size and accessible active sites. Various synthesis approaches have been developed to prepare zeolites with new topology, large pores and functional groups. Large efforts have been made to synthesize new zeolite frameworks from layered precursors by topotactic condensation[2] or an approach called ADOR (assembly, disassembly, organization and reassembly).[3] The layered precursors can be silicates, aluminosilicates or aluminophosphates. Nine zeolite framework types (CAS,[4] NSI,[5] FER,[6] CDO,[2a] PCR,[3] MWW,[7] RRO,[8] RWR,[9] and SDO[10]) have been prepared by the topotactic condensation of silicate layers, five of them (CDO, PCR, NSI, RRO, and RWR) have not yet been obained by direct synthesis. Among these layered precursors, the two-dimensional ferrierite layer related to the FER type zeolite is of particular interest. Four zeolite framework types (FER, CDO, PCR and OKO) can

be synthesized from the ferrierite layers; three of them by stacking the ferrierite layer with different sequences and one (OKO) by connecting the ferrierite layers with single 4-rings.[11]

A novel approach has been employed by Wu's group to synthesize crystalline microporous materials with expanded pore windows from layered zeolite precursors.[12] The layered zeolite precursors were treated with dimethyldiethoxysilane in acid conditions. The silicate layers are connected to each other via siloxane bridges to give a microporous silicate framework. These interlayer expanded zeolites (IEZ) show physical and chemical properties comparable with zeolites, but with larger pore windows and functionalized groups. The structures were investigated extensively by selected area electron diffraction (SAED) and high resolution transmission electron micrsocopy (HRTEM) combined with model building.[12b] The structure models could be deduced from the HRTEM images. However, accurate atomic positions could not be directly obtained from the TEM studies.

Table 1. Crystal data, RED experimental parameters and refinement details for the COE-3 structure ($[Si_{20}O_{38}(CH_3)_4]$, λ=0.0251 Å).

Sample	Dataset 1COE-3	Dataset 2COE-3	Dataset 3COE-3
Structure type		IEZ-CDO	
Tilt range (°)	116.93 (-39.04 ~ 77.89)	109.86 (-66.12 ~ 43.74)	33.37 (-32.9 ~ -66.27)
Tilt step (°)	0.1	0.4	0.2
Exposure time/frame (s)	0.2	0.5	2.0
No. of ED frames	1218	275	187
Crystal system	orthorhombic	orthorhombic	orthorhombic
Space group	*Cmcm*	*Cmcm*	*Cmcm*
Unit cell parameters from RED	a = 7.2 Å b = 21.8 Å c = 13.6 Å α = 89.7° β = 89.5° γ = 90.2°	a = 7.2 Å b = 22.4 Å c = 13.8 Å α = 89.6° β = 88.8° γ = 90.0°	a = 7.3 Å b = 22.4 Å c = 13.6 Å α = 87.9° β = 88.3° γ = 91.2°
Volume (Å³)	2133.8	2213.8	2220.5
Crystal size (µm)	1.0×1.0×0.2	1.1×0.9×0.3	1.5×0.5×0.2
Completeness (%) (d ≥ 1.10 Å)	76.5	67.6	30.5
Reflections collected	1710	1203	529
Observed reflections	649	322	247
Unique reflections (d ≥1.10 Å)	391	309	156
Observed unique reflections	162	127	99
R_{int}	0.1847	0.4242	0.1520

After merging the three datasets, the numbers of unique reflections and observed unique reflections are 418 and 227, respectively. Observed reflections are those that were detected by the peak search using RED. The completeness is 85.4% (d ≥1.10 Å). $R1$ is 0.38 for observed reflections and 0.45 for all data. 38 parameters were refined and 50 distance restraints were applied.

Gies and co-workers also reported a series of interlayer expanded zeolites, COE-n (n = 1-4), by treating the layered zeolite precursors with dichlorodimethylsilane,[13] where COE-2 and COE-4 correspond to the calcined forms of COE-1 and COE-3, respectively. COE-1 and COE-2 were obtained from the layered precursor RUB-39,[13a] while COE-3 and COE-4 from the layered precursor RUB-36.[13b] Al-COE-4 shows unprecedented shape selectivity in decane hydroconversion test.[14]

Structure determination of interlayer expanded zeolites is challenging due to the following reasons: (1) the materials often form as nano- and submicron-sized crystals too small to be studied by single crystal X-ray diffraction; (2) The materials often have poor crystallinity and contain stacking disorder, which lead to low resolution and peak broadening in the PXRD pattern. This can cause ambiguity for the unit cell and space group determination, as well as difficulty in the intensity partitioning of overlapping reflections. This is even more serious if the sample contains impurities. It is generally difficult to perform *ab initio* structure determination of zeolites from low quality PXRD data.

Electron crystallography can overcome the above mentioned limitations of single crystal X-ray diffraction and

PXRD, and is a powerful alternative method for *ab inito* structure determination of complex zeolites.[15] HRTEM has been used for solving structures of unknown zeolites, including one of the most complex zeolite IM-5,[16] and several zeolites containing stacking faults and disorders such as beta polymorph B,[17] ITQ-38,[15c] ITQ-39[18] and SU-78.[19] However, IEZ materials often form very thin plate-like crystals and are electron-beam sensitive due to the weak connections between the layers. In addition, they have preferred orientations in the TEM due to the plate-like morphology of the crystals. It was technically challenging and time-consuming to obtain high quality HRTEM images even for a TEM expert. One such example is demonstrated by Ruan *et al.*.[12]

Recently two new methods have been developed for automated collection and processing of 3D electron diffraction data; the rotation electron diffraction (RED) method[20] developed by our group and the automated diffraction tomography (ADT)[21] developed by Kolb's group in Mainz. The data collection of the RED method is controlled by software *RED* – data collection,[20b] similar to the procedure for single crystal X-ray diffraction but on crystals millions times smaller (~ 100 nm). The *RED* software can be installed in a conventional TEM without any additional hardware. The data

collection can start from an arbitrary crystal orientation without the need of crystal pre-alignment. A series of more than 1000 ED frames can be collected by combining electron beam tilt and goniometer tilt. The 3D reciprocal lattice can be reconstructed by combining the ED frames. The unit cell parameters, space group and diffraction intensities can be extracted from the 3D reciprocal lattice. Structure solution methods used for X-ray diffraction including direct methods (SHELX,[22] SIR[23]), charge flipping (Superflip,[24] Jana[25]) and simulated annealing (FOX,[26] SIR[23]) can be directly applied on the RED or ADT data.

RED and ADT data have been used for soloving novel zeolite structures ITQ-51,[27] PKU-16,[28] and ITQ-43,[29] metal-organic frameworks ZIF-7,[15b] MFU-4,[30] CAU-7,[31] and UiO-66,[32] and covalent organic frameworks COF-320.[33] In this article, we investigate whether the RED method can be used for *ab initio* structure determination of interlayer expanded zeolites. We choose the interlayer expanded microporous silicates COE-3 and COE-4, which were previously solved by model building, geometrically optimized using the program DLS-76[34] and refined by Rietveld refinement against the PXRD data.[13b] PXRD indicates that both structures are monoclinic (space group *Pm*), with $a = 12.2503(3)$ Å, $b = 13.9752(2)$ Å, $c = 7.3850(1)$ Å, and $\beta = 107.33(1)°$ for COE-3 and $a = 12.16985(4)$ Å, $b = 13.95066(3)$ Å, $c = 7.37058(2)$ Å, and $\beta = 107.30(1)°$ for COE-4. The crystal structures of COE-3 and COE-4 are built from the ferrierite layer with a CDO stacking (IEZ-CDO). The linker group connecting the ferrierite layers is $-O-Si(CH_3)_2-O-$ in COE-3 and $-O-Si(OH)_2-O-$ in COE-4. We intended to compare the atomic coordinates obtained from the RED data with those refined by Rietveld refinement[13b].

Experimental

The synthesis of COE-3 and COE-4 has been previously reported.[13b] Samples for the RED data collection were dispersed in absolute ethanol and treated by ultrasonic treatment for 5 min. A droplet of the suspension was transferred onto a carbon-coated copper grid and dried in air. The 3D RED data were collected on a JEOL JEM2100 TEM at 200 kV using the RED - data collection software.[20b] A single-tilt tomography sample holder was used for the data collection, which allows a tilt range from -70° to +70° in the TEM. The ED frames were recorded on a 12-bit Gatan ES500W Erlangshen camera side-mounted at a 35 mm port. Because of the beam damage, low electron dose was applied during the data collection. Even though, it was difficult to collect a complete RED dataset over a large tilt range from one single particle before the crystal was destroyed. Therefore, several datasets from different crystals were collected and merged to obtain a more complete dataset. The beam tilt step was between $0.1 - 0.4°$, and the exposure time was between $0.2 - 2.0$ s per ED frame. The total data collection time was less than 3 hours for all the datasets. Detailed RED data collection and crystallographic information for COE-3 and COE-4 are given in Table 1 and Table 2, respectively.

The data processing was performed using the software *RED-data processing*,[20b] which includes shift correction, peak search, unit cell determination, indexation of reflections and intensity extraction. The rotation axis and reciprocal space sampling (number of pixels per reciprocal Å, pixel*Å) were pre-calibrated using a standard sample. The unit cell was determined from the positions of the diffraction spots detected in the ED frames. The intensity for each reflection was

Table 2. Crystal data, RED experimental parameters and refinement details for the COE-4 structure (($[Si_{20}O_{38}(OH)_4]$, λ=0.0251 Å).

Sample	Dataset 1$_{COE-4}$	Dataset 2$_{COE-4}$
Structure type		IEZ-CDO	
Tilt range (°)	-54.81~53.90	62.94 ~ -56.72
Tilt step (°)	0.4	0.1
Exposure time/frame (s)	1.5	0.6
No. of ED frames	270	1239
Crystal system	orthorhombic	orthorhombic
Space group	*Cmcm*	*Cmcm*
Unit cell parameters from RED	$a = 7.3$ Å $b = 23.0$ Å $c = 14.0$ Å $\alpha = 89.8°$ $\beta = 89.5°$ $\gamma = 90.0°$	$a = 7.3$ Å $b = 22.0$ Å $c = 14.0$ Å $\alpha = 89.6°$ $\beta = 90.9°$ $\gamma = 90.8°$
Volume (Å^3)	2352.6	2242.4
Crystal size (μm)	1.5×1.0×0.2	1.0×0.8×0.3
Completeness (%) (d ≥ 1.02 Å)	75.8	75.3
Reflections collected	2466	2752
Observed reflections	2397	1665
Unique reflections (d ≥ 1.02 Å)	513	477
Observed unique reflections	350	275
R$_{int}$	0.21	0.36

After merging the two datasets, the numbers of unique reflections and observed unique reflections are 513 and 359, respectively. Observed reflections are those that were detected by the peak search using RED. The completeness is 77.2% (d ≥1.02 Å). *R*1 is 0.38 for all observed reflections and 0.44 for all data. There are 35 parameters refined using 49 restraints.
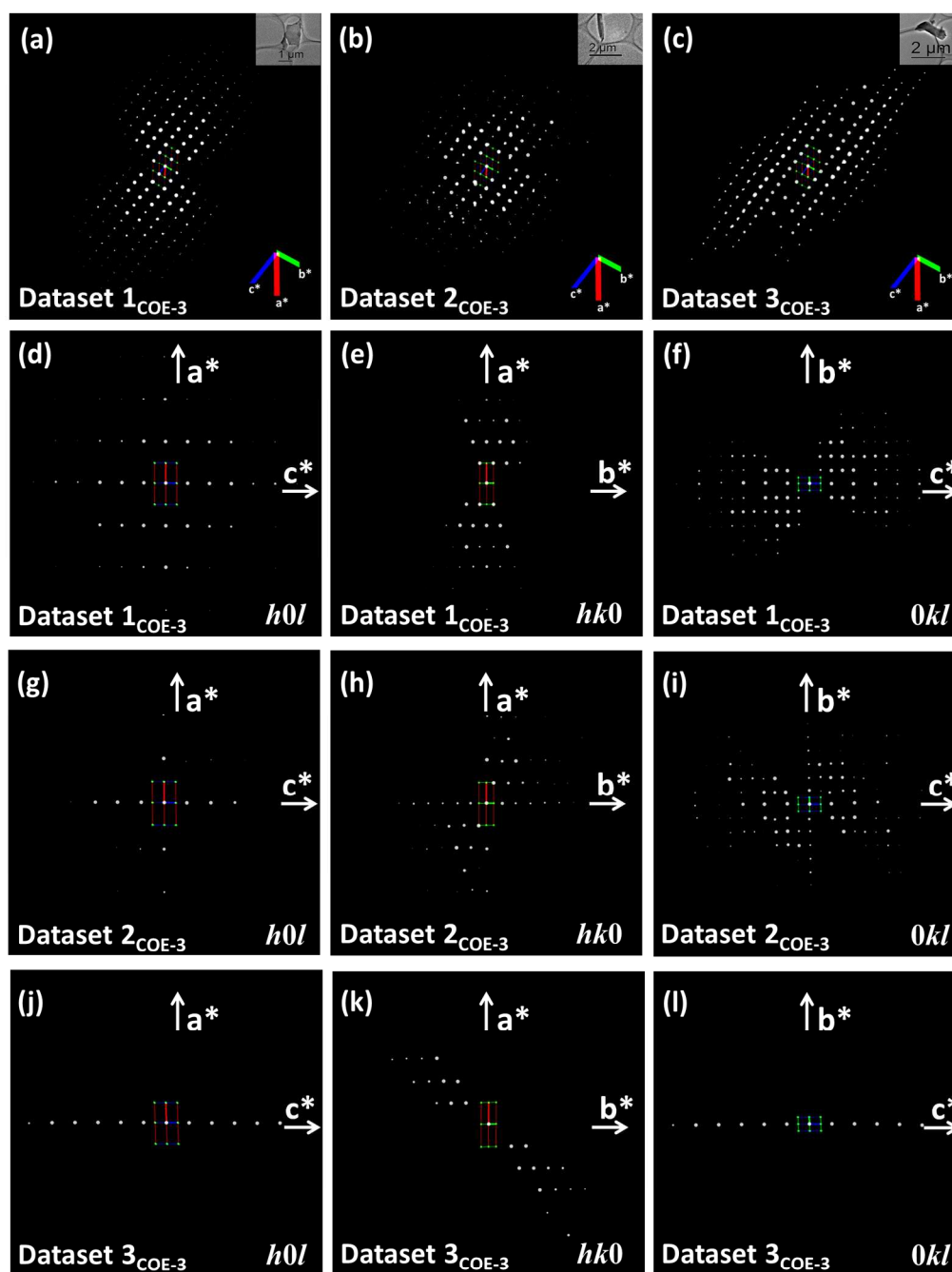
Fig. 1 (a-c) Reconstructed 3D reciprocal lattices of COE-3 from the three RED datasets taken from three crystals. The crystal size and morphology are shown as an insert. (d-f) The 2D slices *h0l*, *hk0* and *0kl* cut from the dataset 1_{COE-3}; (g-i) Three 2D slices *h0l*, *hk0* and *0kl* cut from the dataset 2_{COE-3}; (j-l) three 2D slices *h0l*, *hk0* and *0kl* cut from the dataset 3_{COE-3}. The reciprocal lattice axes are marked, with *a**, *b** and *c** in red, green and blue, respectively.

extracted from the ED frame with the highest intensity value. Reflections that were within the experimental tilt range but too weak to be detected by the RED software were assigned zero intensity. The final list of reflections with the indices and intensities was output to an HKL file in a standard HKLF4 format for SHELX.[22] The structure solution and refinement were performed using SHELX. Atomic scattering factors for electrons were used. Due to the relatively poor data quality, soft restraints were applied to all the Si-O (1.61 Å) and O-O (2.62 Å) distances in the refinement. PXRD patterns of the as-made COE-3 and calcined COE-4 materials were collected on a PANalytical X'Pert Pro diffractometer using the Cu Kα radiation (λ = 1.5418 Å, 45 kV, 40 mA). To prevent preferred orientations, the data collection was carried out in transmission geometry using a capillary sample holder of 0.5 mm in diameter. The Rietveld refinements of COE-3 and COE-4 were

performed using the program TOPAS Academic 4.1. Soft restraints were applied to all the Si-O (1.61 Å) and O-O (2.62 Å) distances. In order to model the electron density generated by the non-framework species in the channels, four carbon atoms and six oxygen atoms representing guest water molecules were added in the channel of COE-3 and COE-4, respectively and their occupancies were refined.

Results and Discussion

Three RED datasets of COE-3 were collected from three different crystals. They contain 1218 (dataset 1_{COE-3}), 275 (dataset 2_{COE-3}), and 187 (dataset 3_{COE-3}) ED frames and cover a tilt range of 116.96°, 109.86° and 33.37°, respectively. For each dataset, the ED frames obtained at different tilt angles were combined into a 3D reciprocal lattice, see Figs. 1a-c. The three datasets are complementary to each other, covering different parts of the reciprocal lattice. Figs. 1d-f, Figs. 1g-i and Figs. 1j-l show the three 2D $h0l$, $hk0$ and $0kl$ slices cut from the dataset 1_{COE-3}, 2_{COE-3} and 3_{COE-3}, respectively. Due to the thin plate-like morphology of the crystals, it was difficult to obtain the $0k0$ reflections along the b^*-axis. Only dataset 2_{COE-3} contains the $0k0$ reflections (Fig. 1h). 1714 reflections (391 unique) were obtained from dataset 1_{COE-3}, 1203 reflections (309 unique) from dataset 2_{COE-3} and 529 reflections (156 unique) from dataset 3_{COE-3}. Despite of the data incompleteness, the unit cell parameters of COE-3 could be obtained from the reconstructed 3D reciprocal lattice from each of the three RED datasets, as given in Table 1. Dataset 1_{COE-3} covers the largest tilt angle

among the three datasets. The corresponding unit cell parameters show the smallest deviation (0.46°) from the orthorhombic unit cell, which indicates that COE-3 is orthorhombic. The same trend was also observed in the study of calcined silicalite-1, where we compared the effects of different data collection parameters, such as tilt step, tilt range and resolution, on the unit cell parameters.[35] Compared to the severe peak overlap in the PXRD data of COE-3 (Fig. 4a), reflections in the 3D RED data are separated so that the space group determination is straight forward. The 2D $h0l$, $hk0$ and $0kl$ slices cut from each of the three datasets are shown in Figs. 1d-f. The possible space groups of COE-3 are $Cmc2_1$ (No.36), $C2cm$ (No.40) or $Cmcm$ (No.63), as deduced from the reflection conditions observed from Fig. 1: hkl: $h+k=2n$; $h0l$: $h=2n$, $l=2n$; $hk0$: $h+k=2n$; $0kl$: $k=2n$; $h00$: $h=2n$; $0k0$: $k=2n$; $00l$: $l=2n$. Because most of the zeolite structures in the IZA Database of Zeolite Structures are centrosymmetric, we choose the centrosymmetric space group $Cmcm$ for further structure solution. It should be mentioned that a few diffuse streaks are observed along the b^*-axis (see Fig. S1), indicating the presence of stacking disorders of the ferrierite layers. Since the intensity of the diffuse streaks is not very strong, only the intensities of discrete diffraction spots at the reciprocal lattice points were used for structure determination.

The structure of COE-3 could not be solved from any of the single datasets. Thus the three datasets from different crystals with different initial orientations were merged in order to obtain a more complete dataset (418 unique reflections, of which 227 observed). The structure of COE-3 was solved by direct
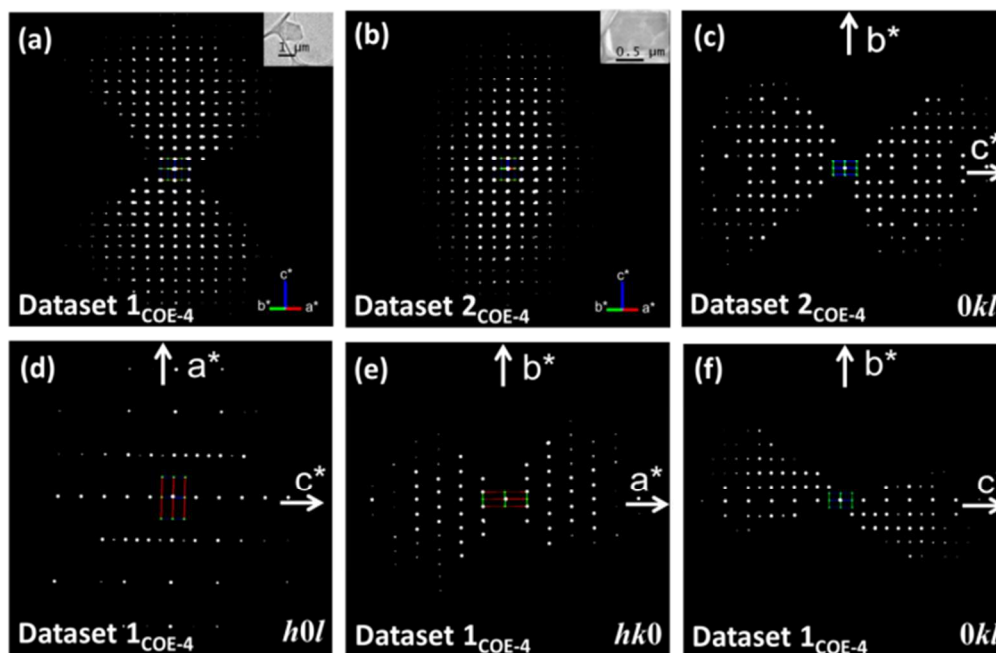
Fig. 2 (a-b) Reconstructed 3D reciprocal lattices of COE-4 (a) dataset 1_{COE-4} and (b) dataset 2_{COE-4} taken from two crystals. The crystal size and morphology are shown as an insert. (c) 2D slices $0kl$ cut from the dataset 2_{COE-4}. (d-f) Three 2D $h0l$, $hk0$ and $0kl$ slices cut from the dataset 1_{COE-4}. The reciprocal lattice axes are marked, with a^*, b^* and c^* in red, green and blue, respectively.
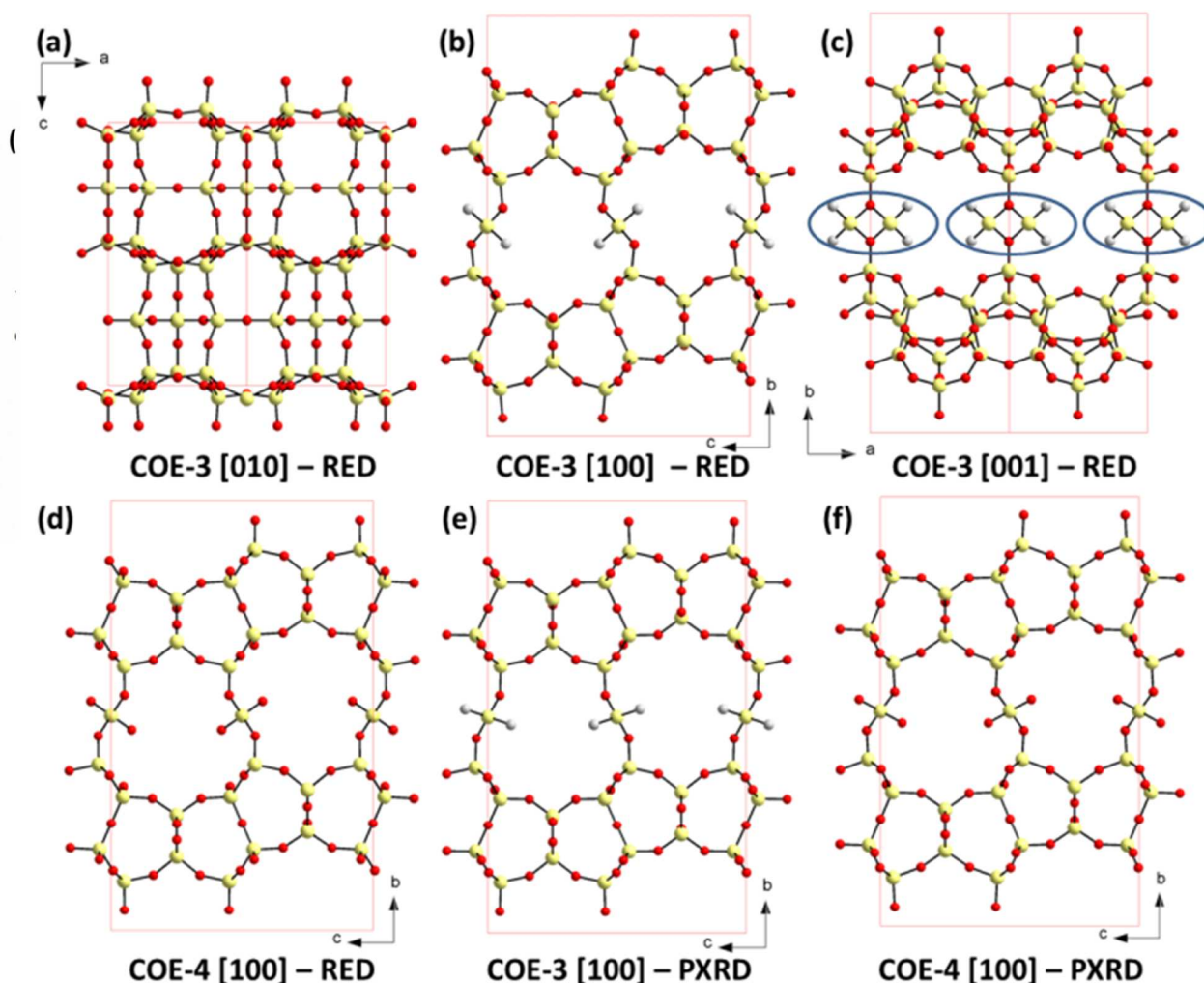
Fig. 3 (a–c) The structure of COE-3 determined by RED. (a) The ferrierite layer viewed along the [010] direction, perpendicular to the layer. (b–c) The 3D structure viewed along the (b) [100] and (c) [001] directions. The ellipses in (c) indicate the disorder of the $Si(CH_2)$ group; only one of the $Si(CH_2)$ group in each ellipse is present. (d) The 3D structure of COE-4 determined by RED. (e-f) The 3D structure of (e) COE-3 and (f) COE-4 refined against the PXRD data. The Si, O and C atoms are shown in yellow, red and grey, respectively.

methods from the merged dataset using the program SHELX. All the five Si atoms including the bridging Si atom between the ferrierite layers and 5 out of 8 O atoms in the asymmetric unit could be found. The three missing O atoms (O6 atom located in the inversion centre, O4 and O8 coordinated with Si4) were added according to the geometry of SiO_4 tetrahedra. Since solid state NMR indicates that the linker groups carry two methyl substituents,[13b] a carbon atom representing the $-CH_3$ group was also added according to the tetrahedral coordination of the Si atom (Si5) in the linker groups. The structure including the linker group $SiO_2(CH_3)_2$ was further refined against the RED data, (Table 1). The refinement converged to a $R1$ value of 0.38 for the 227 observed reflections. The structure model is shown in Figs. 3a-c.

COE-4 is the calcined form of the as-made COE-3 material. Two datasets were collected from two different COE-4 crystals, which contain 270 (dataset 1_{COE-4}) and 1239 (dataset 2_{COE-4}) ED frames and cover the tilt range of 108.71° and 119.66°,

respectively. The reconstructed 3D reciprocal lattice is shown in Fig. 2. 2466 reflections (513 unique) were obtained from dataset 1_{COE-4} (Fig. 2a), while 2752 reflections (477 unique) were obtained from dataset 2_{COE-4} (Fig. 2b). The reflection conditions of dataset 1_{COE-4} (Figs. 2d-f) agree with the centrosymmetric space group *Cmcm* (No. 63), which was chosen for the structure solution. The two datasets are complementary to each other, as seen from the 3D reciprocal lattices reconstructed from the two datasets (Figs. 2a-b). As shown in Fig. 2c, the completeness of the $0kl$ plane in the dataset 2_{COE-4} is higher than that in the dataset 1_{COE-4}. The structure of COE-4 could be solved by direct methods from the intensities merged from these two datasets using the program SHELX. All five Si atoms and 6 out of 9 O atoms in the asymmetric unit were found. The three missing O atoms (O6 located in the inversion centre, O8 coordinated with Si4, and O9 in the OH-group coordinated with Si5) were added according to the geometry of the SiO_4 tetrahedra. The structure
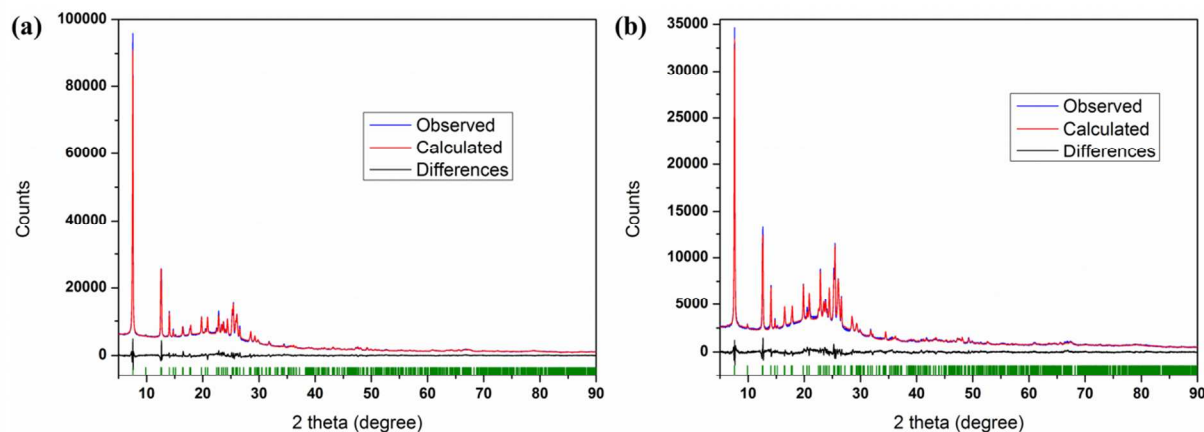
Fig. 4 X-ray Rietveld refinement plots of (a) COE-3 and (b) COE-4. The observed, calculated and difference curves are in blue, red and grey, respectively. The vertical bars indicate the positions of Bragg peaks (λ = 1.5418 Å).

including the linker group $SiO_2(OH)_2$ was further refined against the RED data (Table 2). The refinement converged to a $R1$ value of 0.38 for the 359 observed reflections. The structure model is shown in Fig. 3d.

The framework structures of COE-3 and COE-4 are very similar (Figs. 3b and 3d); both are built of the ferrierite layers constructed exclusively from 5-rings (Fig. 3a). The layers are connected by the linker group $SiO_2(CH_3)_2$ in COE-3 and $SiO_2(OH)_2$ in COE-4 to form the three-dimensional framework. The largest shift of Si atoms between COE-3 and COE-4 was 0.12 Å, with an average shift of 0.07 Å. The average shift for oxygen and carbon was 0.21 Å, with the largest deviation for O3 (0.75 Å) which is located at the mirror plane.

The framework structures of COE-3 and COE-4 can be regarded as an interlayer expanded CDO zeolite (IEZ-CDO). The CDO zeolite was obtained by topotactic condensation of PREFER-layers from a crystalline hydrous layer RUB-36. After the insertion of the linker groups between the ferrierite layers, the pore opening of the channels increased from 8-ring (in the CDO type zeolite) to 10-ring along a- and c-axes to form the frameworks with two-dimensional 10-ring channels, as shown in Figs. 3b-d. The methyl groups in COE-3 point towards the 10-ring channels, making them hydrophobic. After the calcination, the channels in COE-4 became hydrophilic due to the transformation of methyl groups into hydroxyl groups. The linker groups in both COE-3 and COE-4 are located near the mirror plane perpendicular to the a-axis so that they are disordered into two sites with the maximum occupancy of 0.5 each, as indicated in Fig. 3c. The occupancy of the linker group was refined against the RED data, which converged to 0.22 for COE-3 and 0.12 for COE-4. Due to the high $R1$ values attributed to the electron-beam damage and dynamical effects, we are not sure about these occupancies. However, we believe that the structure of the ferrierite layer and connectivity of the layers via the linker groups are correct.

Although the space group and unit cell parameters of COE-3 and COE-4 obtained from the RED data are different from those previously reported,[13b] their framework topologies are the same. In order to further confirm the structures, we performed

Rietveld refinement of the COE-3 and COE-4 structures obtained from RED against the PXRD data collected from the same samples. The crystal data and structure refinement details are given in Table S1. The Rietveld refinement plots are presented in Fig. 4. The final refinement converged to R_{wp} of 0.043 for COE-3 and 0.049 for COE-4. The bond lengths of Si-O are in the range of 1.581(4)-1.655(5) Å for COE-3 and 1.573(6)-1.617(6) Å for COE-4. The Si-O-Si angles between the four connected SiO_4 tetrahedra are in the range of 135.6(2)°-159.0(12)° for COE-3 and 129.6(3)°-165.3(5)° for COE-4, except for the Si3-O6-Si3 angle where O6 is at an inversion centre so that the Si3-O6-Si3 angle is 180°. The occupancy of the bridging Si5 atom was refined and converged to 0.41 for COE-3 and 0.32 for COE-4. The final structures of COE-3 and COE-4 refined against PXRD data are shown in Figs. 3e-f. The effective pore diameters along the c- and a-axis are 5.3 Å × 4.7 Å and 5.5 Å × 5.2 Å for COE-3 and 5.3 Å × 4.7 Å and 5.6 Å × 4.9 Å, respectively, as shown in Figs. S2 and S3. Representative bond distances and angles of COE-3 and COE-4 are given in Table S2 and Table S3, respectively.

The atomic positions of the framework atoms refined against RED data and PXRD data are compared, see Table S4 for COE-3 and Table S5 for COE-4. For COE-3, the average deviation is 0.06 Å for the Si atoms and 0.22 Å for the O atoms. The carbon (-CH$_3$) position belonging to the linker group deviates mostly, by 0.56 Å, which is expected due to the disorder. For COE-4, the average deviation is 0.04 Å for the Si atoms and 0.13 Å for the O atoms. The oxygen (-OH) position belonging to the linker group deviates by 0.10 Å. This indicates that the accuracy of the Si positions obtained from the RED data is three times better than that of the oxygen positions. The CH_3 group in COE-3 shows the largest deviation, indicating that its position was not well located from the RED data. We noticed that the discrepancies between the structures refined against the RED and PXRD data are significantly smaller for COE-4 than those for COE-3. This means that the structure model of COE-4 obtained from the RED data is more accurate than that of COE-3. This is reasonable because the RED data for COE-4 contains more reflections (359 for COE-4 and 227

for COE-3) and lower d-values (1.02 Å for COE-4 and 1.10 Å for COE-3).

Our structure models are also compared to the previously reported ones, which were determined as monoclinic and had the space group *Pm*. The main difference of the previous model from the model of the present work is that the neighbouring ferrierite layers are slightly shifted along the *c*-axis, and no disorder of the linker groups is present in the previous work. The disorder in the present model may be due to the use of the high symmetry *Cmcm* in the refinement. Since the quality of the current data is not good enough to allow the structure refinement in a lower symmetry, we are not sure whether the linker groups would be ordered if a lower symmetry would have been used. Furthermore, the samples used in this work were synthesized in Germany, while those used in the previous work were made in China. The corresponding PXRD patterns between the two sample batches show some differences, which may result in the different unit cells and space groups.

Conclusions

We have demonstrated the power of the new rotation electron diffraction (RED) method for *ab initio* structure determination of two interlayer expanded zeolites COE-3 and COE-4. Single crystal RED data was collected from particles of a few hundred nanometers in size. The unit cell parameters and space group were directly obtained from the 3D RED data. Both COE-3 and COE-4 are electron-beam sensitive, several RED datasets were collected from different crystals, merged together for the structure determination. All Si atoms and most of the oxygen atoms could be directly located by direct methods. The structures could be refined using the RED data. COE-3 and COE-4 are built of ferrierite-type layers pillared by (-O-Si(CH$_3$)$_2$-O-) and (-O-Si(OH)$_2$-O-) linker groups, respectively. The layers are stacked with a CDO type stacking to form an IEZ-CDO type structure. The structures contain 2D intersecting 10-ring channels running in parallel to the ferrierite layers. The final structure models refined against the RED data deviate from those refined against the PXRD data on average by less than 0.06 Å for the Si atoms and 0.22 Å for the O atoms. This shows that the RED method can give a very good single crystal structure from sub-micron sized crystals of layered inorganic solids.

Acknowledgements

Notes and references

a Inorganic and Structural Chemistry and Berzelii Centre EXSELENT on Porous Materials, Department of Materials and Environmental Chemistry, Stockholm University, Stockholm, SE-10691, Sweden. *Fax: +46 8 15 21 87; Tel: +46 8 16 23 89; E-mail: xzou@mmk.su.se*
b Institut für Geologie, Mineralogie und Geophysik, Ruhr-Universität, Bochum, 44780 Bochum, Germany
c Key Lab of Applied Chemistry of Zhejiang Province, Department of Chemistry, Zhejiang University, Hangzhou 310007, China.

1. (a) M. E. Davis, Nature, 2002, **417**, 813-821; (b) M. E. Davis and R. F. Lobo, Chem. Mater., 1992, **4**, 756-768.
2. (a) T. Ikeda, Y. Akiyama, Y. Oumi, A. Kawai and F. Mizukami, Angewandte Chemie International Edition, 2004, **43**, 4892-4896; (b) Z. Zhao, W. Zhang, P. Ren, X. Han, U. Müller, B. Yilmaz, M. Feyen, H. Gies, F.-S. Xiao, D. De Vos, T. Tatsumi and X. Bao, Chem. Mater., 2013, **25**, 840-847.
3. W. J. Roth, P. Nachtigall, R. E. Morris, P. S. Wheatley, V. R. Seymour, S. E. Ashbrook, P. Chlubná, L. Grajciar, M. Položij, A. Zukal, O. Shvets and J. Čejka, Nat. Chem., 2013, **5**, 628-633.
4. B. Marler, M. Camblor and H. Gies, Microporous Mesoporous Mater., 2006, **90**, 87-101.
5. S. Zanardi, A. Alberti, G. Cruciani, A. Corma, V. Fornes and M. Brunelli, Angew. Chem. Int. Ed., 2004, **43**, 4933-4937.
6. (a) L. Schreyeck, P. Caullet, J. Mougenel, J. Guth and B. Marler, Microporous Mater., 1996, **6**, 259-271; (b) L. Schreyeck, P. Caullet, J. Mougenel, J. Guth and B. Marler, Stud. Surf. Sci. Catal., 1997, **105**, 1949-1956.
7. M. E. Leonowicz, J. A. Lawton, S. L. Lawton and M. K. Rubin, Science, 1994, **264**, 1910-1913.
8. Y. X. Wang, H. Gies, B. Marler and U. Müller, Chem. Mater., 2004, **17**, 43-49.
9. B. Marler, N. Ströter and H. Gies, Microporous Mesoporous Mater., 2005, **83**, 201-211.
10. T. Moteki, W. Chaikittisilp, A. Shimojima and T. Okubo, J. Am. Chem. Soc., 2008, **130**, 15780-15781.
11. E. Verheyen, L. Joos, K. Van Havenbergh, E. Breynaert, N. Kasian, E. Gobechiya, K. Houthoofd, C. Martineau, M. Hinterstein and F. Taulelle, Nat. Mater., 2012, **11**, 1059-1064.
12. (a) P. Wu, J. Ruan, L. Wang, L. Wu, Y. Wang, Y. Liu, W. Fan, M. He, O. Terasaki and T. Tatsumi, J. Am. Chem. Soc., 2008, **130**, 8178-8187; (b) J. Ruan, P. Wu, B. Slater, Z. Zhao, L. Wu and O. Terasaki, Chem. Mater., 2009, **21**, 2904-2911.
13. (a) H. Gies, U. Müller, B. Yilmaz, T. Tatsumi, B. Xie, F.-S. Xiao, X. Bao, W. Zhang and D. D. Vos, Chem. Mater., 2011, **23**, 2545-2554; (b) H. Gies, U. Mu□ller, B. Yilmaz, M. Feyen, T. Tatsumi, H. Imai, H. Zhang, B. Xie, F.-S. Xiao and X. Bao, Chem. Mater., 2012, **24**, 1536-1545.

14. B. Yilmaz, U. Müller, B. Tijsebaert, D. De Vos, B. Xie, F.-S. Xiao, H. Gies, W. Zhang, X. Bao and H. Imai, Chem. Commun., 2011, **47**, 1812-1814.

15. (a) T. Willhammar and X. Zou, Z. Kristallogr., 2013, 228, 11-27; (b) T. Willhammar, Y. Yun and X. Zou, Adv. Funct. Mater., 2014, **24**, 182-199; (c) M. Moliner, T. Willhammar, W. Wan, J. González, F. Rey, J. L. Jorda, X. Zou and A. Corma, J. Am. Chem. Soc., 2012, **134**, 6473-6478.

16. (a) J. Sun, Z. He, S. Hovmöller, X. Zou, F. Gramm, C. Baerlocher and L. B. McCusker, Z. Kristallogr., 2010, **225**, 77-85; (b) C. Baerlocher, F. Gramm, L. Massüger, L. B. McCusker, Z. He, S. Hovmöller and X. Zou, Science, 2007, **315**, 1113-1116.

17. A. Corma, M. Moliner, Á. Cantín, M. J. Díaz-Cabañas, J. L. Jordá, D. Zhang, J. Sun, K. Jansson, S. Hovmöller and X. Zou, Chem. Mater., 2008, **20**, 3218-3223.

18. T. Willhammar, J. Sun, W. Wan, P. Oleynikov, D. Zhang, X. Zou, M. Moliner, J. Gonzalez, C. Martínez and F. Rey, Nat. Chem., 2012, **4**, 188-194.

19. Z.-B. Yu, Y. Han, L. Zhao, S. Huang, Q.-Y. Zheng, S. Lin, A. Córdova, X. Zou and J. Sun, Chem. Mater., 2012, **24**, 3701-3706.

20. (a) D. Zhang, P. Oleynikov, S. Hovmöller and X. Zou, Z. Kristallogr., 2010, **225**, 94-102; (b) W. Wan, J. Sun, J. Su, S. Hovmoller and X. Zou, J. Appl. Crystallogr., 2013, **46**, 1863-1873.

21. (a) U. Kolb, T. Gorelik, C. Kübel, M. Otten and D. Hubert, Ultramicroscopy, 2007, **107**, 507-513; (b) U. Kolb, T. Gorelik and M. Otten, Ultramicroscopy, 2008, **108**, 763-772; (c) E. Mugnaioli, T. Gorelik and U. Kolb, Ultramicroscopy, 2009, **109**, 758-765.

22. G. M. Sheldrick, Acta Crystallogr. A, 2007, **64**, 112-122.

23. M. C. Burla, R. Caliandro, M. Camalli, B. Carrozzini, G. L. Cascarano, C. Giacovazzo, M. Mallamo, A. Mazzone, G. Polidori and R. Spagna, J. Appl. Crystallogr., 2012, **45**, 357-361.

24. L. Palatinus and G. Chapuis, J. Appl. Crystallogr., 2007, **40**, 786-790.

25. V. Petricek, Dusek,M. and Palatinus,L., Jana2006. The crystallographic computing system. Institute of Physics, Praha, Czech Republic., 2006.

26. V. Favre-Nicolin and R. Cerny, J. Appl. Crystallogr., 2002, **35**, 734-743.

27. R. Martínez-Franco, M. Moliner, Y. Yun, J. Sun, W. Wan, X. Zou and A. Corma, Proc. Natl. Acad. Sci., 2013, **110**, 3749-3754.

28. W. Hua, H. Chen, Z.-B. Yu, X. Zou, J. Lin and J. Sun, Angew Chem. Int. Ed., 2014, DOI: 10.1002/anie.201309766.

29. J. Jiang, J. L. Jorda, J. Yu, L. A. Baumes, E. Mugnaioli, M. J. Diaz-Cabanas, U. Kolb and A. Corma, Science, 2011, **333**, 1131-1134.

30. D. Denysenko, M. Grzywa, M. Tonigold, B. Streppel, I. Krkljus, M. Hirscher, E. Mugnaioli, U. Kolb, J. Hanss and D. Volkmer, Chem. Eur. J., 2011, **17**, 1837-1848.

31. M. Feyand, E. Mugnaioli, F. Vermoortele, B. Bueken, J. M. Dieterich, T. Reimer, U. Kolb, D. de Vos and N. Stock, Angew. Chem. Int. Ed., 2012, **51**, 10373-10376.

32. L. Zhu, D. Zhang, M. Xue, H. Li and S. Qiu, CrystEngComm, 2013, **15**, 9356-9359.

33. Y.-B. Zhang, J. Su, H. Furukawa, Y. Yun, F. Gándara, A. Duong, X. Zou and O. M. Yaghi, J. Am. Chem. Soc., 2013, **135**, 16336-16339.

34. C. Baerlocher, A. Hepp, W. M. Meier, DLS-76: A program for the simulation of crystal structures by geometric refinement, Lab. f. Kristallographie, ETH, Zürich, 1978.

35. J. Su, E. Kapaca, L. Liu, V. Georgieva, W. Wan, J. Sun, V. Valtchev, S. Hovmöller and X. Zou, Microporous Mesoporous Mater., 2013, **189**, 115-125.
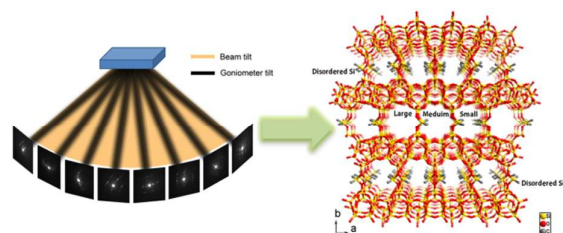
Rotation electron diffraction (RED) combines beam tilt and goniometer tilt to get single crystal electron diffraction data, which has been used for *ab initio* structure determination of interlayer expanded zeolites.